

MGCD0103, a selective histone deacetylase inhibitor, coameliorates oligomeric A β_{25-35} -induced anxiety and cognitive deficits in a mouse model

Hei-Jen Huang¹ | Hsin-Yu Huang² | Hsiu Mei Hsieh-Li² 

¹Department of Nursing, Mackay Junior College of Medicine, Nursing and Management, Taipei, Taiwan

²Department of Life Science, National Taiwan Normal University, Taipei, Taiwan

Correspondence: Hsiu Mei Hsieh-Li, Department of Life Science, National Taiwan Normal University, Taipei 11677, Taiwan (hmhsieh@ntnu.edu.tw).

Funding information

Ministry of Science and Technology (Taiwan), Grant/Award Number: MOST 103-2325-B-003-003, MOST 104-2325-B-003-003 and MOST 105-2325-B-003-003

Summary

Aims: Recently, histone deacetylase (HDAC) inhibitors are considered a possible therapeutic strategy in Alzheimer's disease (AD). However, HDACi treatments exhibit diverse functions with unfavorable effects in AD. Thus, the development of selective HDACi without side effects is urgently needed.

Methods: HDACi, namely, BML210, MGCD0103, PXD101, and Droxinostat, were screened in mouse hippocampal primary cultures incubated with oligomeric A β_{25-35} (50 μ mol/L). MGCD0103 was chosen for in vivo tests and was intraperitoneally injected into C57BL/6J mice (0.5 mg/kg, once per day) for 4 weeks following an intra-hippocampal CA1 injection of oligomeric A β_{25-35} . Brain samples were collected for pathological analyses after the behavioral analyses including open-field test (OFT), elevated plus maze (EPM), Y-maze, and Morris water maze (MWM).

Results: Among the HDACi, MGCD0103 exhibited significant neuroprotection against the A β toxicity in primary cultures. MGCD0103 coattenuated cognitive deficits and anxiety against A β damage in mice. MGCD0103 further ameliorated pathological features such as the levels of acetylated histone 3 at Lys 9 site (H3K9) and α -tubulin, synaptophysin, A β , tau protein phosphorylation, and serotonergic neuron loss against A β toxicity. Furthermore, chronic MGCD0103 treatment did not show liver or kidney toxicity in mice.

Conclusions: These results reveal MGCD0103 could be a potential therapeutic agent against AD.

KEYWORDS

anxiety, cognition, histone deacetylase inhibitor, MGCD0103, oligomeric A β_{25-35}

1 | INTRODUCTION

Alzheimer's disease (AD) is the most common neurodegenerative disease and the major cause of dementia in the aging population. The major pathological features of AD are extracellular senile plaques of aggregated A β and hyperphosphorylated tau protein-enriched intraneuronal neurofibrillary tangles (NFT) in brain tissue,

including in the temporal lobe, limbic system, and neocortex.^{1,2} However, the development of therapeutic AD drugs, including anti-A β , anti-tau protein phosphorylation, antioxidants, and anti-inflammatory agents, has been disappointing for the multifactorial elements of AD.³⁻⁶ Therefore, ongoing investigations and promising new ways of understanding the puzzle pieces of AD are urgently needed.

This is an open access article under the terms of the Creative Commons Attribution-NonCommercial License, which permits use, distribution and reproduction in any medium, provided the original work is properly cited and is not used for commercial purposes.

© 2018 The Authors. *CNS Neuroscience & Therapeutics* Published by John Wiley & Sons Ltd

Environmental factors such as stress, anxiety, and epigenetic alterations have been reported to play a significant role in the pathogenesis of sporadic or late-onset AD (LOAD).⁷⁻¹⁰ Epigenetic mechanisms regulate gene expression through histone acetylation and DNA methylation of normal nucleotide sequences of a gene. There are four families of histone deacetylase (HDAC) enzymes encoded from both the human and rodent genomes: class I (including HDAC 1-3 and 8), class IIa (HDAC 4, 5, 7, and 9), class IIb (HDAC 6 and 10), and class IV (HDAC11).¹¹ Evidence further suggests that the development of the epigenetic drugs may provide a new direction in AD.^{12,13} Previous experimental treatments with pan-HDAC inhibitors (nonselective HDAC inhibitors, HDACi), such as sodium butyrate, trichostatin A, suberoylanilide hydroxamic acid, or sodium phenylbutyrate, have shown promising therapeutic effects in animal models of AD and neuropsychiatric disorders.¹⁴⁻¹⁶ However, pan-HDACi should be used with caution because of the unfavorable side effects that they can cause in the brain.¹⁷ Therefore, the development of selective HDACi with the reduction in unwanted side effects needs to be addressed in AD treatments.

In this study, we first identified a lead compound selected from four HDACi that would serve as an appropriate chemical probe to test its therapeutic potential in AD treatment. In mouse primary hippocampal neuronal cultures, we found that MGCD0103 showed neuroprotective effects superior to those of the three other HDACi. MGCD0103, an isotype-selective HDACi, has been clinically evaluated for the treatment of tumors¹⁸ and has also shown a promising pharmacological profile as an anticancer agent, including reliability, tolerance, and safety.^{19,20} Therefore, the potential therapeutic effects and mechanisms of MGCD0103 were characterized in mice received with an acute bilateral intrahippocampal CA1 injection of oligomeric A β_{25-35} . Our data show that MGCD0103 can effectively and safely attenuate the anxiety and cognitive deficits associated with an increase in acetylated histone and nonhistone (α -tubulin) proteins and can ameliorate the pathological features of AD, including A β deposition, tau protein phosphorylation, gliosis, and loss of serotonergic neurons and synapse-related proteins. Based on these results, we suggest that MGCD0103 could be developed as a novel therapeutic approach for AD.

2 | METHODS

2.1 | Animals and ethics statement

All experimental procedures using mice received specific approval from the Institutional Animal Care and Use Committee (IACUC) of the National Taiwan Normal University, Taipei, Taiwan (Permit Number: 104010). C57BL/6J mice were purchased from the National Breeding Centre for Laboratory Animals. In vivo animal experiments were carried out with mature (12-week-old) males, and pregnant females were utilized for primary hippocampal cultures. Mice were maintained on a 12 hours light/dark cycle with a constant ambient temperature (20-25°C) and relative humidity (60%), with food and water available ad libitum. Every effort was made to minimize any suffering to the animals.

2.2 | Preparation of A β_{25-35} oligomer and HDAC inhibitors

A β_{25-35} peptides were purchased from Sigma (SI-A4559, Saint Louis, MO 63103, USA), solubilized in sterile distilled water (3 mg/mL), and stored at -20°C until use. For in vitro use, A β_{25-35} peptides were diluted to 50 μ mol/L with physiological saline and aggregated by incubation at 37°C for 4 days before use, as previously described.²¹ For in vivo use, A β_{25-35} peptides were diluted to 10 nmol/L with physiological saline and aggregated by incubation at 37°C for 7 days before bilateral injection into the hippocampal CA1 subregion (i.c.). The IC₅₀ values of four HDACi (BML210; MGCD0103; PXD101; Droxinostat) were determined by an MTT assay (see Supporting Information) using a SH-SY5Y neuroblastoma cell line (Table S1). HDACi were diluted with DMSO and applied to the primary culture at three different concentrations (Table S1; low, medium, and high).

2.3 | Administration of MGCD0103

The elimination half-life in plasma of MGCD0103 is 7-11 hours.²²⁻²⁴ Chronic intrathecal delivery (4 weeks Alzet minipumps) of MGCD0103 (30 or 60 nmol/d) was administrated into the spinal cord of nerve injury rats.²⁵ In addition, four HDACi (BML210, MGCD0103, PXD101, Droxinostat) in three different doses (high, medium, and low dose based on IC₅₀) were screened using mouse primary hippocampal neuronal culture (Figure S1). We found that the neuroprotective effect of MGCD0103 was superior to the other three HDACi, especially in low and high doses (Figure S1). Furthermore, the performance in neuroprotection of MGCD0103 in high dose was better than low dose (Figure S2). Therefore, the in vivo dose of MGCD0103 (0.5 mg/kg; Biovision) was determined based on the results of the primary hippocampal neuronal cultures (high dose) and evidence of its ability to penetrate the BBB.^{23,24} MGCD0103 was first dissolved in DMSO (40 mg/mL) and then diluted with a mixed buffer (saline:Kolliphor, 4:1; Kolliphor (C5135; Sigma-Aldrich)) to 0.5 mg/kg before intraperitoneal injection (i.p.) in mice once a day for 28 days following stereotaxic surgery. The toxicity of chronic MGCD0103 injections in liver and kidney was assessed by hematoxylin and eosin (HE) staining (Table S2).

2.4 | Experimental design

Six days after adaption in an animal room, mice were anesthetized on day 7 by an intraperitoneal injection of avertin (0.4 g/kg body weight; Sigma, Saint Louis, MO 63103, USA) and mounted in a stereotaxic frame (David Kopf Instruments, Tujunga, CA, USA). 3 μ L of either saline or oligomeric A β_{25-35} (10 nmol/L) was injected bilaterally into the hippocampal CA1 with a 10.0 μ L Hamilton syringe using the following coordinates: anteroposterior -0.23 mm from bregma, mediolateral \pm 0.2 mm from midline, depth -0.15 mm from skull. After surgery recovery, mice were administered MGCD0103 (0.5 mg/kg, i.p.) for 28 days (days 8-36). Mice were divided into four groups: (a) saline (i.c.)/saline (i.p.); (b) saline (i.c.)/MGCD0103 (i.p.); (c) A β_{25-35} (i.c.)/saline (i.p.);

TABLE 1 List of primary antibodies in immunohistochemistry and Western blot

| Antibody | Species | Supplier | WB dilution | IHC dilution |
|---------------------|---------|----------------------------------|-------------|--------------|
| Iba-1 | Rabbit | Wako, Osaka, Japan | | 1:1000 |
| GFAP | Mouse | Millipore, Temecula, CA, USA | | 1:1000 |
| 5-HT | Rat | Millipore, Temecula, CA, USA | | 1:200 |
| ChAT | Rabbit | Millipore, Temecula, CA, USA | | 1:1000 |
| TH | Rabbit | Millipore, Temecula, CA, USA | | 1:1000 |
| 6E10 | Mouse | Covance, Princeton, NJ, USA | | 1:1000 |
| pS202Tau | Rabbit | AnaSpec, San Jose, CA, USA | | 1:1000 |
| pS9GSK3 β | Rabbit | Cell Signaling, Danvers, MA, USA | 1:1000 | |
| GSK3 β | Rabbit | Cell Signaling, Danvers, MA, USA | 1:1000 | |
| pT216GSK3 β | Mouse | Millipore, Temecula, CA, USA | 1:1000 | |
| pT181Tau | Rabbit | Millipore, Temecula, CA, USA | 1:1000 | |
| pS396Tau | Rabbit | Invitrogen, Rockford, USA | 1:1000 | |
| pT205Tau | Rabbit | Invitrogen, Rockford, USA | 1:1000 | |
| Total tau (HT7) | Mouse | Thermo, Rockford, IL, USA | 1:500 | |
| BACE1 | Rabbit | Cell Signaling, Danvers, MA, USA | 1:1000 | |
| Synaptophysin | Mouse | Abcam, Cambridge, UK | 1:1000 | |
| PSD95 | Goat | Santa Cruz, Dallas, TX, USA | 1:1000 | |
| ERK | Rabbit | Cell Signaling, Danvers, MA, USA | 1:1000 | |
| pERK | Rabbit | Cell Signaling, Danvers, MA, USA | 1:1000 | |
| CDK5 | Mouse | Millipore, Temecula, CA, USA | 1:1000 | |
| pCDK5 | Mouse | Santa Cruz, Dallas, TX, USA | 1:1000 | |
| IDE | Rabbit | Abcam, Cambridge, UK | 1:1000 | |
| NEP | Mouse | Santa Cruz, Dallas, TX, USA | 1:1000 | |
| AcH3K9 | Rabbit | Cell signaling, Danvers, MA, USA | 1:1000 | |
| Histone 3 | Rabbit | Millipore, Temecula, CA, USA | 1:1000 | |
| A α -tubulin | Mouse | Santa Cruz, Dallas, TX, USA | 1:1000 | |
| α -tubulin | Mouse | Sigma, Bath, UK | 1:5000 | |
| β -actin | Mouse | Millipore, Temecula, CA, USA | 1:2000 | |

or (d) A β_{25-35} (i.c.)/MGCD0103 (i.p.). During MGCD0103 treatment, mice underwent a series of behavioral tests: an open-field test (OFT) (day 24), an elevated plus maze (EPM) test (day 26), a Y-maze test (day 28), and a Morris water maze (MWM) test (days 30-36). After behavioral testing, mice were sacrificed for pathological analyses on day 37.

2.5 | Evaluation of behavioral tasks

During the MGCD0103 treatment period, mice were evaluated in OFT, EPM, Y-maze, and MWM tests. Before the behavioral tests, mice were acclimatized to the behavioral testing room for 30 minutes. All experiments were completed between 7:00 and 17:00, and the behavioral performance of the mice was recorded and analyzed by an automatic tracking system (EthoVision-XT; Noldus, Wageningen, Netherlands). The test box was sequentially cleaned with 70% and 30% ethanol before the next mouse was introduced to the box.

2.6 | Open-field test

The OFT was conducted as previously described.⁷ Mice were individually placed in the central zone (15 \times 15 cm) of a white acrylic box (30 \times 30 \times 30 cm) and then recorded for 10 minutes with a video camera. Anxiety-like phenotypes were evaluated as a decrease in the time spent in the center of the open field arena.

2.7 | Elevated plus maze

The maze consisted of four arms (30 \times 5 cm) extending out from a central square (10 \times 10 cm), where two arms had 15-cm high walls and were 50 cm above floor level. Mice were placed in the central square facing one of the open arms, and their activity was video tracked for 5 minutes. The total time that mice spent in the open arms was determined and used as an index of anxiety.

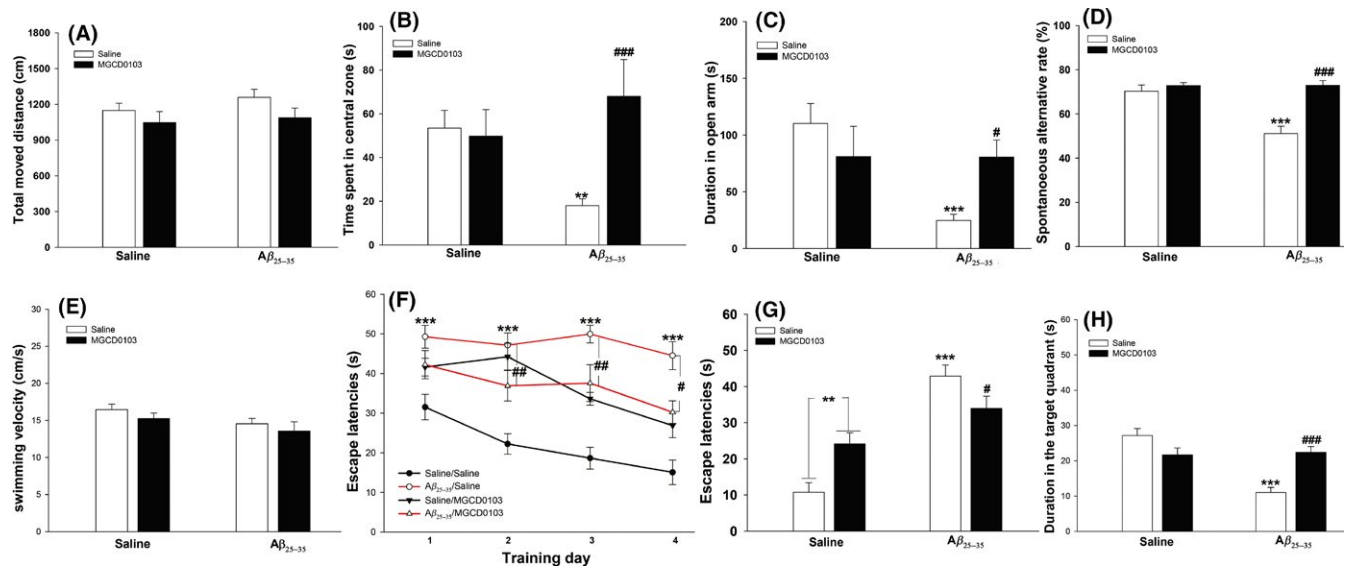


FIGURE 1 Effects of MGCD0103 on Anxiety and Cognitive Deficits in Oligomeric $A\beta_{25-35}$ -Treated Mice. A, Motor activity in an open-field test (OFT). There was no difference among the four groups. B-C, Time spent in the central zone in the OFT and overall time spent in the open arms of the EPM, which were evaluated as indexes of anxiety. MGCD0103 reduced anxiety in oligomeric $A\beta_{25-35}$ -treated mice. D, The spontaneous alternation rate of mice in the Y-maze was measured as an index of short-term memory. MGCD0103 reduced the short-term memory deficits induced by oligomeric $A\beta_{25-35}$. E, Swimming velocity was measured on the pretraining day of the MWM task. No differences were identified among the four groups of mice. F, The learning profiles of the four groups of mice during the 4 training days. MGCD0103 improved learning abilities in the oligomeric $A\beta_{25-35}$ group. G, Latency to identify the platform during the testing phase. MGCD0103 treatment reduced the time for the mice to climb onto the platform in the oligomeric $A\beta_{25-35}$ group but increased spatial learning acquisition impairments in the saline group. H, Results of long-term memory retrieval testing. Oligomeric $A\beta_{25-35}$ impaired long-term memory retrieval, and MGCD0103 attenuated this deficit. Data are presented as the mean \pm SEM for each group. $n = 12-15$. *, compared to the saline (i.c.)/saline (i.p.) group; #, compared to the oligomeric $A\beta_{25-35}$ (i.c.)/saline (i.p.) group (#, $P < 0.05$; **, $P < 0.01$; ***, $P < 0.001$)

2.8 | Y-maze

The Y-maze apparatus consisted of 3 identical symmetric arms ($46 \times 3 \times 17$ cm) with white acrylic walls. The Y-maze task was conducted as described.²⁶ Each mouse was placed in the central space and allowed to explore freely for 8 minutes, while their rates of spontaneous alternations were assessed as an indicator of short-term memory. Arm entry was defined as the entry of all four paws into one arm. Spontaneous alternation percentage was calculated by the equation: [successive entries/(total arm entries - 2) \times 100].

2.9 | Morris water maze

The spatial learning and memory abilities of the mice were assessed through the MWM task as previously described.⁷ Before the training phase, the swimming ability of the mice was tested on day 30. Mice that floated in the pool were not enrolled in the task. In the training phase, each mouse underwent four 1-minute trials to locate the hidden platform on 4 consecutive days (days 31-34). The time to climb onto the hidden platform was recorded as the escape latency. On day 35, three testing trials were performed as an index of spatial learning acquisition. Twenty-four hours after the last testing trial (day 36),

a probe test was performed. The platform was removed from the pool, and each mouse was allowed to swim freely for 60 seconds. The amount of time spent in the quadrant of the original platform location was calculated as an index of long-term spatial memory.

2.10 | Immunohistochemistry (IHC)

Immunohistochemistry staining was performed as previously described.⁷ Mice ($n = 3-5$ per group) were deeply anesthetized with avertin (0.4 g/kg body weight) and then transcardially perfused with normal saline followed by 4% paraformaldehyde (PFA) in 0.1 mol/L phosphate buffer. Harvested brain tissues were postfixed in the same solution at 4°C for 4 hours and then dehydrated in a graded series of sucrose solutions until they were fully permeated. Frozen brain sections were cut 30- μ m thick in a coronal plane using a cryostat microtome (CMS3050S, Leica Microsystems, Nussloch, Germany), and IHC staining was performed on 3-4 sections per mouse. Slices were incubated with the primary antibodies as Table 1 overnight at room temperature and the appropriate biotinylated secondary antibodies (1:200, Vector Laboratories, Burlingame, CA, USA) for 1 hour at room temperature, followed by incubation with an avidin-biotin-peroxidase complex (ABC kit; Vector Laboratories, Burlingame, CA, USA) for 1 hour at room temperature. After rinsing with PBS (10 minutes, three

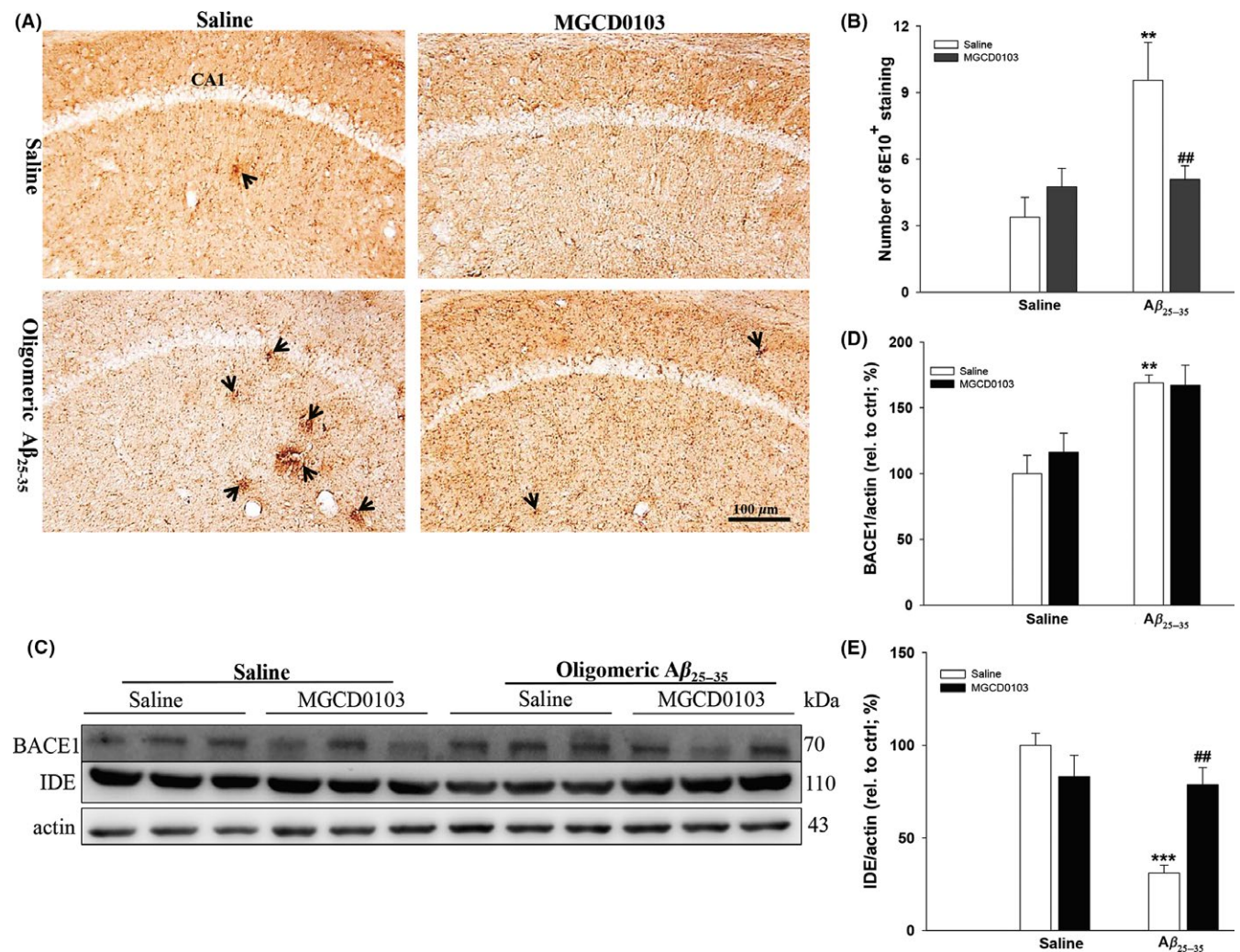


FIGURE 2 Effects of MGCD0103 on Aβ Levels in Oligomeric Aβ₂₅₋₃₅ Mice. (A) Representative immunohistochemical staining of amyloid deposits in the mouse hippocampus using 6E10 antibody. Scale bar = 100 μm. The arrowheads indicate positive staining (n = 3-4 per group). (B) Quantitative results of immunohistochemical staining. Representative Western blots (C) and quantitative densitometry results for BACE1 (D) and IDE (E) expression levels. β-actin was used as an internal control. The quantitative data are presented as the mean ± SEM for each group (n = 3-5 per group). *, compared to the saline (i.c.)/saline (i.p.) group; #, compared to the oligomeric Aβ₂₅₋₃₅ (i.c.)/saline (i.p.) group (**, ##, P < 0.01; ***, P < 0.001)

changes), the sections were incubated with a diaminobenzidine (DAB) kit (Vector Laboratories, Burlingame, CA, USA). Slices were stained and observed using a light microscope (Leica, Wetzlar, Germany). Images were obtained using Image-Pro Plus 5.1 (Image-Pro Plus Media Cybernetics, Washington, MD, USA), and the threshold intensity was manually set at a constant value for all images. Pixel counts were derived from the average of three adjacent sections per animal.

2.11 | Western blot

Three to five mouse hippocampi from each group were collected and homogenized in RIPA lysis buffer (1:2, w/v). An aliquot of 20 μg protein was used for Western blot analysis as previously described.⁷ After blocking, membranes were incubated with the primary antibodies listed in Table 1 at 4°C for 16 hours. Next, membranes were incubated

with the secondary antibodies corresponding to the type of primary antibody (1:10 000, Amersham Pharmacia Biotech, Piscataway, NJ, USA) for 2 hours at room temperature and developed using an ECL kit (ECL, Amersham, MA, USA). β-actin was used as a loading control. Blots were scanned by a LAS-4000 chemiluminescence detection system (Fujifilm, Tokyo, Japan), and the quantification of band density was performed using Gel-Pro Analyzer software (GelPro32, version 4.0; Media Cybernetics, Inc., Rockville, MD, USA).

2.12 | Statistical analysis

Data are shown as the mean ± SEM. Data were analyzed by SPSS 20.0 statistics software (Armonk, New York, USA) using one-way ANOVA or Student's t tests. P < 0.05 was considered to be statistically significant.

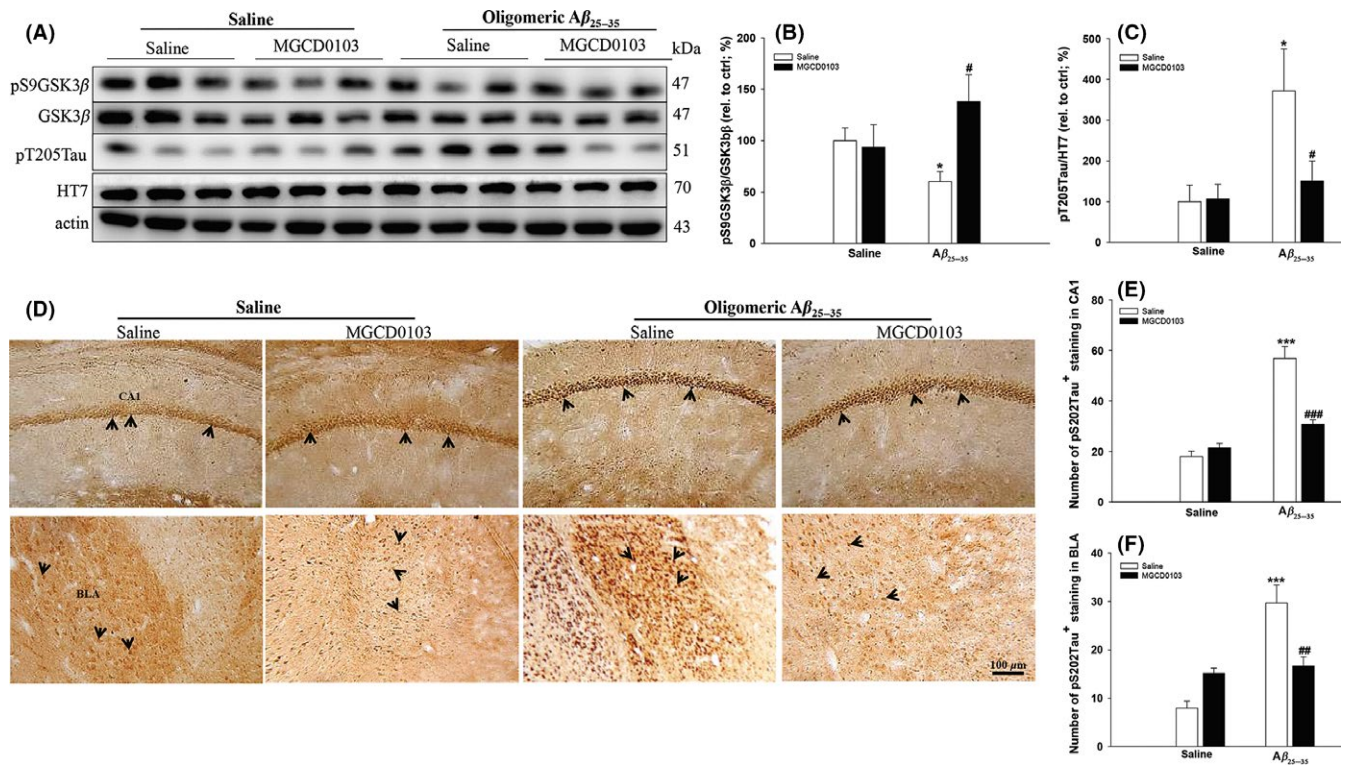


FIGURE 3 Effects of MGCD0103 on Tau Phosphorylation-Related Proteins in Oligomeric Aβ₂₅₋₃₅ Mice. (A) Representative Western blots and quantitative densitometry results for the ratios of pS9GSK3β/GSK3β (B) and pT205Tau/HT7 (total tau) (C). β-actin was used as an internal control. (D) Representative immunohistochemical staining of pS202Tau in the CA1 subregion of the hippocampus and the BLA. Scale bar = 100 μm. The arrowheads indicate positive staining of pS202Tau (n = 3-4 per group). Quantitative results for pS202Tau in the CA1 subregion of the hippocampus (E) and the BLA (F). *, compared to the saline (i.c.) /saline (i.p.) group; #, compared to the oligomeric Aβ₂₅₋₃₅ (i.c.) /saline (i.p.) group (*, #, P < 0.05; ##, P < 0.01; ***, ###, P < 0.001)

3 | RESULTS

3.1 | MGCD0103 attenuated the anxiety and cognitive deficits induced by oligomeric Aβ₂₅₋₃₅

To investigate whether MGCD0103 attenuated the anxiety and cognitive deficits induced by oligomeric Aβ₂₅₋₃₅, we performed OFT, EPM, Y-maze, and MWM experiments. The total distance travelled in the OFT was not different between the four groups (Figure 1A), which indicates that mice from all groups had normal motor activity. Despite this normal motor activity, the oligomeric Aβ₂₅₋₃₅ significantly lowered the cumulative time spent in the center zone compared to the intra-hippocampal injection of saline (P < 0.01; Figure 1B). However, the administration of MGCD0103 significantly increased the cumulative time spent in the center zone compared to the saline treatment of mice who received oligomeric Aβ₂₅₋₃₅ injections (P < 0.001; Figure 1B). In the EPM task, the oligomeric Aβ₂₅₋₃₅-treated group showed significantly reduced total time spent in the open arms compared to the saline-treated group (P < 0.001; Figure 1C). MGCD0103 treatment induced a significant increase in the cumulative time spent in the open arms compared to saline treatment for mice who received oligomeric Aβ₂₅₋₃₅ injections (P < 0.05; Figure 1C). These results suggest that the treatment of MGCD0103 ameliorated the anxiety caused by oligomeric Aβ₂₅₋₃₅ injections.

In addition, the oligomeric Aβ₂₅₋₃₅-treated group exhibited significantly reduced short-term memory compared with the

saline-treated group in the Y-maze test (P < 0.001; Figure 1D). However, the recognition memory performance inhibited by oligomeric Aβ₂₅₋₃₅ was effectively restored by the i.p. administration of MGCD0103 (P < 0.001; Figure 1D). The treatment with MGCD0103 recovered the short-term memory damage induced by oligomeric Aβ₂₅₋₃₅.

In the MWM task, the time for the mice to reach the hidden platform was compared among the four groups (Figure 1E-H). First, no significant difference in swimming speeds was found among the four groups of mice (Figure 1E). In the 4-day positioning navigation test, the escape latency of the mice was not significantly decreased by oligomeric Aβ₂₅₋₃₅ treatment following training days 1-4 (F_{3,59} = 0.68, P > 0.05; Figure 1F). Compared with the saline-treated group, the group administered Aβ₂₅₋₃₅ had a significant longer escape latency on all 4 days (P < 0.001; Figure 1F), indicating that the administration of Aβ₂₅₋₃₅ induced a learning deficit. This deficit was ameliorated by the administration of MGCD0103 on days 2-4 (P < 0.05-0.01; Figure 1F).

On the 5th day of the MWM (testing phase), mice from the Aβ₂₅₋₃₅-treated group spent more time locating the platform than did saline-treated mice (P < 0.001; Figure 1G), indicating deficits in memory acquisition. The administration of MGCD0103 significantly improved the memory acquisition damage induced by oligomeric Aβ₂₅₋₃₅ (P < 0.05; Figure 1G). In the saline-treated group, MGCD0103 treatment significantly impaired memory acquisition

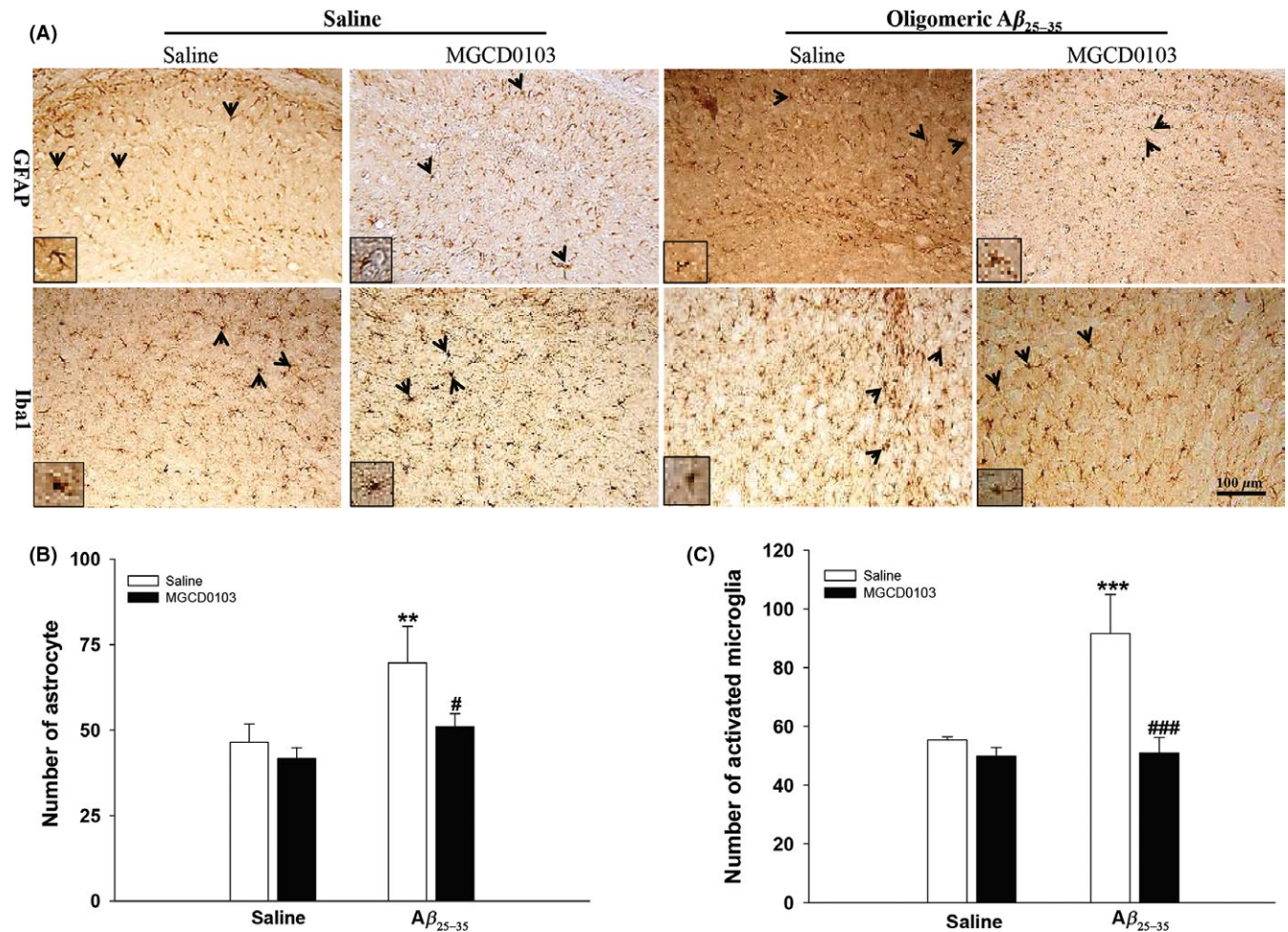


FIGURE 4 Effects of MGCD0103 on Gliosis in Oligomeric A β_{25-35} Mice. (A) Representative immunohistochemical staining of astrocytes and microglia using anti-GFAP and anti-Iba1 antibodies in mouse hippocampal tissue. Scale bar = 100 μ m. The arrowheads indicate positive staining of activated microglia and astrocytes, which are magnified in the insets of each figure ($n = 3-4$ per group). Quantitative results for astrocytes (B) and activated microglia (C). *, compared to the saline (i.c.)/saline (i.p.) group; #, compared to the oligomeric A β_{25-35} (i.c.)/saline (i.p.) group (#, $P < 0.05$; **, $P < 0.01$; ***, ###, $P < 0.001$)

($P < 0.01$; Figure 1G), which suggests that MGCD0103 should not be used before the onset of disease. On the 6th day of the MWM (probe phase), deficits in memory retention were observed in the oligomeric A β_{25-35} -treated group ($P < 0.001$; Figure 1H), and the administration of MGCD0103 improved memory retention ($P < 0.001$; Figure 1H). The results obtained from these different behavioral tasks suggest that the administration of MGCD0103 attenuated the anxiety and cognitive deficits in oligomeric A β_{25-35} -treated mice.

3.2 | MGCD0103 decreased A β levels via increasing the expression levels of IDE in oligomeric A β_{25-35} -treated mice

Immunohistochemistry staining revealed the extensive A β deposition in the hippocampus of oligomeric A β_{25-35} -treated mice compared to saline-treated mice ($P < 0.01$; Figure 2A,B). Furthermore, the deposition of A β was significantly decreased in the hippocampus of the MGCD0103-treated group under oligomeric A β_{25-35} conditions ($P < 0.01$, Figure 2A,B). In addition, BACE1, IDE, and NEP

were also evaluated to elucidate the effects of MGCD0103 on the metabolism of A β . The levels of BACE1 in the oligomeric A β_{25-35} -treated group were significantly higher than those of the saline-treated group ($P < 0.01$; Figure 2C,D); however, there was no change following the administration of MGCD0103 (Figure 2C,D). In addition, MGCD0103 markedly enhanced the reduced expression of IDE induced by oligomeric A β_{25-35} ($P < 0.01$; Figure 2C,E). There was no difference in the levels of NEP among the four groups of mice (data not shown). These results indicated that MGCD0103 administration may mitigate A β deposition by increasing the levels of IDE.

3.3 | MGCD0103 attenuates the increased expression of pTau seen in oligomeric A β_{25-35} -treated mice

Cyclin-dependent kinase 5 (CDK5) and GSK3 β are major kinases that participate in the pathological hyperphosphorylation of tau in both 3xTg-AD mice and the human brain.^{27,28} Therefore, we used IHC staining and Western blot analyses to evaluate the

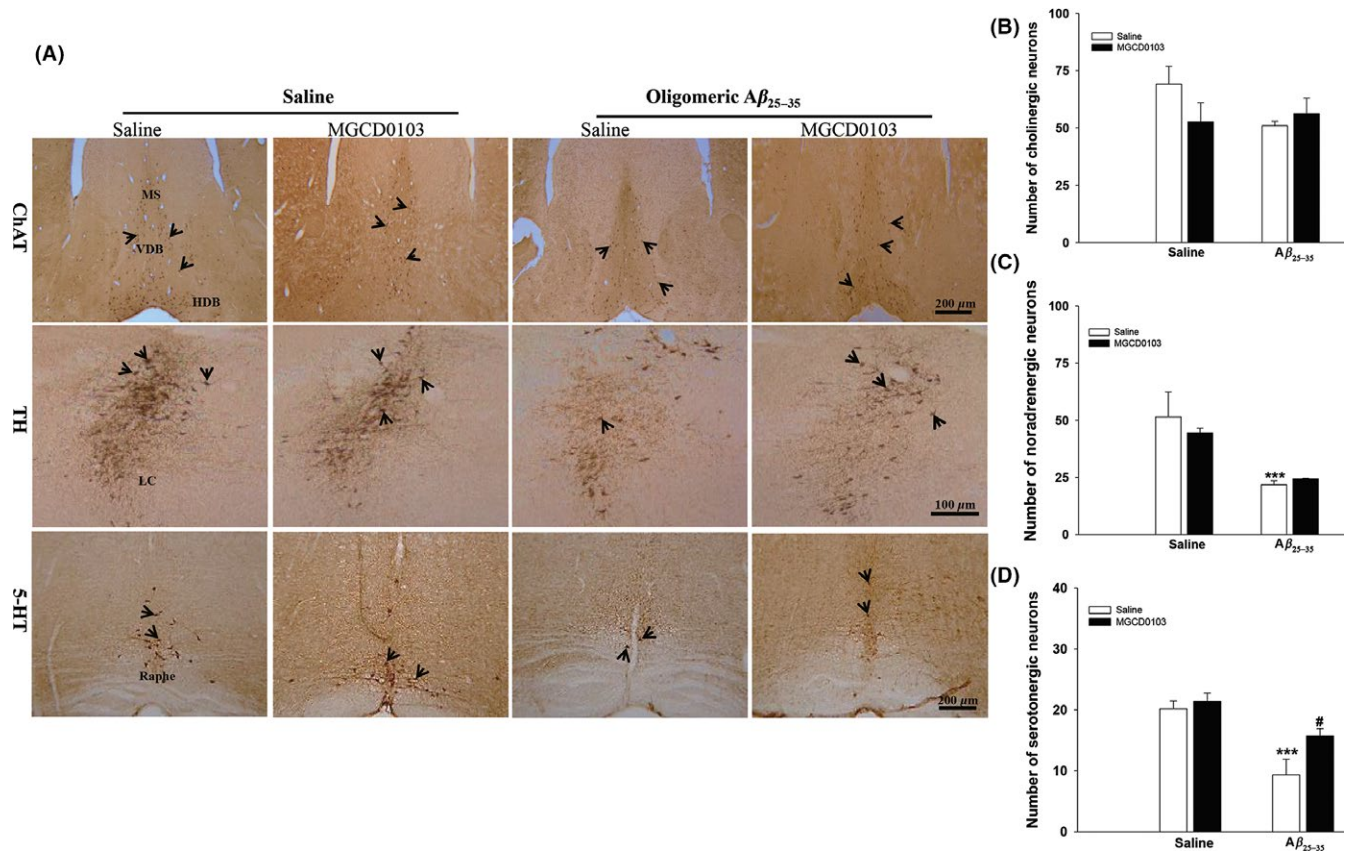


FIGURE 5 Effects of MGCD0103 on Neuronal Loss in Oligomeric Aβ₂₅₋₃₅ Mice. (A) Representative immunohistochemical staining of cholinergic neurons in the MS/DB, noradrenergic neurons in the LC, and serotonergic neurons in the raphe nucleus. Scale bar = 200 μm for cholinergic and serotonergic neurons and 100 μm for noradrenergic neurons. The arrowheads indicate positive staining (n = 3-4 per group). Quantitative results of cholinergic neurons in the MS/DB (B), noradrenergic neurons in the LC (C), and serotonergic neurons in the raphe nucleus (D). *, compared to the saline (i.c.)/saline (i.p.) group; #, compared to the oligomeric Aβ₂₅₋₃₅ (i.c.)/saline (i.p.) group (#, *P* < 0.05; ***, *P* < 0.001)

expression levels of pTau, CDK5, and GSK3β in the hippocampus and basolateral amygdala (BLA) of mice. Injections of oligomeric Aβ₂₅₋₃₅ significantly reduced the levels of pS9GSK3β (inactive form of GSK3β; *P* < 0.05; Figure 3A,B) and increased the levels of pTau at the T205 (*P* < 0.05; Figure 3A,C) and S202 sites (*P* < 0.001; Figure 3D,E) in the hippocampus and the S202 site in the BLA (*P* < 0.001; Figure 3D,F) compared to injections of saline. Moreover, the administration of MGCD0103 significantly reversed these changes in pTau-related proteins induced by the Aβ₂₅₋₃₅ oligomer in the hippocampal and BLA regions (*P* < 0.05-0.001; Figure 3). However, the levels of CDK5, a second critical tau kinase, were not modulated by MGCD0103 treatment (data not shown). Therefore, MGCD0103 treatment increased the levels of pS9GSK3β expression that accompanied the reduction in tau protein phosphorylation at the T205 and S202 sites in oligomeric Aβ₂₅₋₃₅-treated mice.

3.4 | MGCD0103 reduced the gliosis induced by oligomeric Aβ₂₅₋₃₅

Gliosis is a common pathological process in AD²⁹; thus, the modifications in gliosis were evaluated. First, the expression of GFAP (a marker

for astrocytes) and Iba1 (a marker for microglia) proteins was measured by IHC staining. Staining results in the hippocampal region revealed that Aβ₂₅₋₃₅-inoculated mice had significantly increased levels of GFAP compared to saline-inoculated mice (*P* < 0.01; Figure 4A,B). These effects were ameliorated by systemic treatment with MGCD0103 (*P* < 0.05; Figure 4A,B). In addition, the number of activated microglia in the hippocampal area showed increased levels of activated microglia in the oligomeric Aβ₂₅₋₃₅-treated group compared to the levels in the saline-treated group (*P* < 0.001; Figure 4A,C); this effect was counteracted by systemic treatment with MGCD0103 (*P* < 0.001; Figure 4A,C). Therefore, we suggest that the administration of MGCD0103 reduced the gliosis that was elevated by the toxicity of oligomeric Aβ₂₅₋₃₅.

3.5 | MGCD0103 ameliorated the loss of serotonergic neurons in oligomeric Aβ₂₅₋₃₅-treated mice

The progression of cognitive deficits is closely reflected by neuronal loss.³⁰ The staining results showed that the numbers of noradrenergic in locus coeruleus (LC) and serotonergic neurons in raphe nucleus but not cholinergic neurons in medial septal nucleus/diagonal band (MS/DB) were significantly decreased in Aβ₂₅₋₃₅-treated mice compared to the numbers in saline-treated mice (*P* < 0.001; Figure 5A-D). The number of serotonergic neurons was protected by

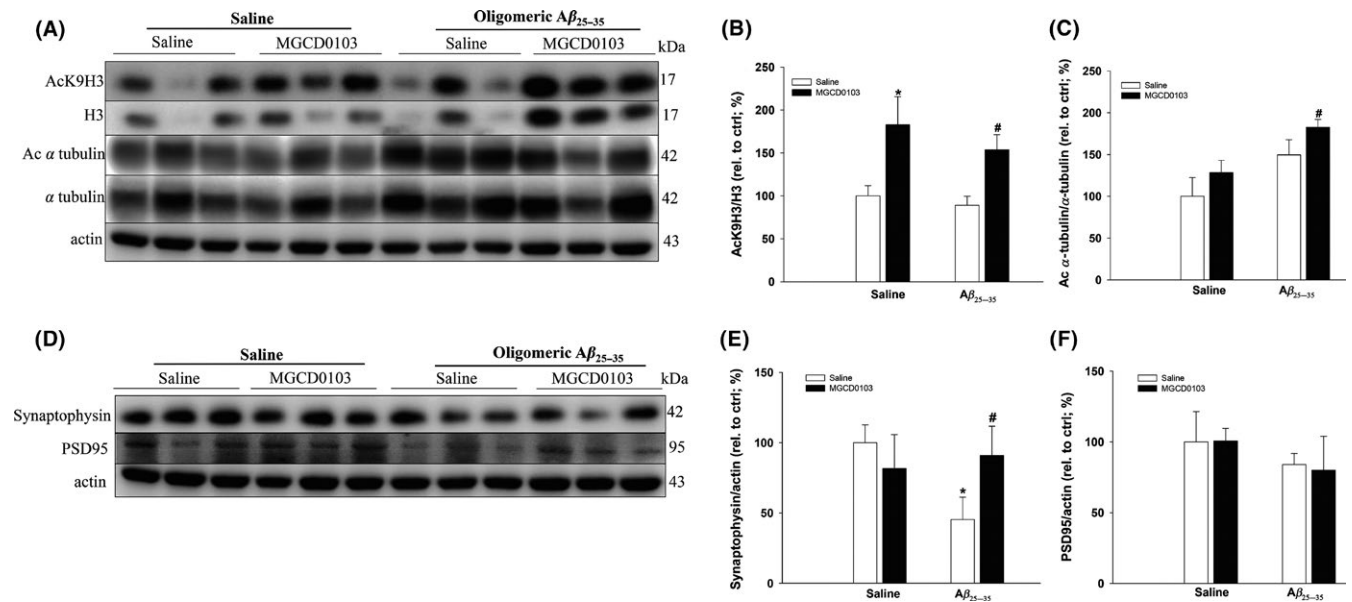


FIGURE 6 Effects of MGCD0103 on the Levels of Acetylated Histone 3, α -Tubulin, and Synaptophysin Expression in Oligomeric $A\beta_{25-35}$ Mice. Representative Western blots (A) and quantitative densitometry results for the ratios of AcK9H3/H3 (B) and Ac α -tubulin/ α -tubulin (C). Representative Western blots (D) and quantitative densitometry results for the expression levels of synaptophysin (E) and PSD95 (F). β -actin was used as an internal control. The quantitative data are presented as the mean \pm SEM for each group ($n = 3-5$ per group). *, compared to the saline (i.c.)/saline (i.p.) group; #, compared to the oligomeric $A\beta_{25-35}$ (i.c.)/saline (i.p.) group (*, #, $P < 0.05$)

systemic MGCD0103 treatment under oligomeric $A\beta_{25-35}$ conditions ($P < 0.05$; Figure 5A,D).

3.6 | MGCD0103 increased the levels of acetylated histone 3 and α -tubulin and the expression of synaptophysin

In this study, we found that the levels of acetylated H3 at the Lys 9 site (ACh3K9) and α -tubulin were not different in the groups treated with oligomeric $A\beta_{25-35}$ or saline (Figure 6A-C). However, MGCD0103 significantly increased the acetylation of H3K9 in saline- and oligomeric $A\beta_{25-35}$ -treated mice ($P < 0.05$, Figure 6A,B) and α -tubulin (nonhistone) in oligomeric $A\beta_{25-35}$ -treated mice ($P < 0.05$, Figure 6A,C). Evidence also shows that synaptic disruptions, such as decreases in the levels of the presynaptic protein synaptophysin and the postsynaptic protein PSD-95, have been observed in the AD brain.^{31,32} We thus investigated whether synaptic proteins were altered. MGCD0103 significantly increased the expression levels of synaptophysin in oligomeric $A\beta_{25-35}$ -treated mice ($P < 0.05$, Figure 6D,E). However, no changes in PSD-95 were detected following MGCD0103 treatment (Figure 6D,F).

4 | DISCUSSION

In the present study, we demonstrated that the systemic chronic administration of MGCD0103 attenuated anxiety and cognitive deficits and AD-associated neuropathological markers in oligomeric $A\beta_{25-35}$ -treated mice. In addition, chronic treatment of MGCD0103 did not

show toxicity in liver and kidney of mice. These results indicate that MGCD0103 may be a potential therapeutic agent against AD.

In this study, bilateral intrahippocampal injection of oligomeric $A\beta_{25-35}$ increased anxiety, cognitive dysfunction, $A\beta$ deposition, IDE expression level, tau protein phosphorylation, neuroinflammation, and loss of noradrenergic and serotonergic neurons and decreased the synaptophysin expression level in mice. AD is a complex multifactorial disease. Mounting evidence has demonstrated that the accumulation of soluble $A\beta$ oligomers played an important role in AD pathogenesis.^{33,34} The accumulation of $A\beta$ in the brain initiates a cascade of events, including neuroinflammatory response, oxidative injury, and kinases/phosphatase activities, which lead patients to present with the symptoms of dementia.³⁵ Intrahippocampal injection of oligomeric $A\beta$ via stereotaxic is widely used to generate an animal model for AD study.³⁶⁻⁴⁰ Evidence also demonstrated that the platform of intrahippocampal $A\beta_{25-35}$ injection can be used to evaluate the cognitive effects of drug in animals.³⁸ In addition, it is reported that $A\beta_{1-40}$, the major component of $A\beta$ deposition, which is soluble and nontoxic and is easily converted by brain proteases to truncated toxic fragments, $A\beta_{25-35/40}$. This may account for the lag between $A\beta$ deposition and neurodegeneration in AD.⁴¹ Therefore, mice received an acute bilateral intrahippocampal $A\beta_{25-35}$ injection were established as an AD animal model in the study.

The administration of MGCD0103 attenuated the anxiety and cognitive deficits that accompanied a decrease in serotonergic neuron loss in the raphe nucleus of oligomeric $A\beta_{25-35}$ -treated mice. The most common manageable side effects of MGCD0103 therapy at doses 70-110 mg (orally 3 times a week in 28-day cycles) in tumor therapy are fatigue, nausea, and vomiting.^{22,23} The dose (0.5 mg/

kg once daily) we applied to the mice in this study was much lower than the doses in the treatment of tumors. The dose could be even lowered when it is applied to patients with AD according to the body surface area (BSA) normalization method.⁴² In addition, there is no difference in motor activity in the groups of mice with or without the treatment of MGCD0103 during this study. Furthermore, we did not observe significant lesion in pathological examination of livers and kidneys of the sacrificed mice at the end of treatment. These results reveal the low toxicity of MGCD0103 for the AD model. Psychological symptoms of dementia are an integral part of AD.^{43,44} Early evidence shows marked serotonergic neuron loss, predominantly in the raphe nucleus, in patients with AD.⁴⁵ Evidence also suggests that a dysregulation of the serotonergic system induces anxiety-like behaviors.⁴⁶ Previous immunohistochemical evidence also suggests that serotonergic fibers have dense terminals in the basolateral complex of the amygdala.⁴⁷ In addition, HDACi such as valproic acid (VPA) and trichostatin A (TSA) modulate the activity of serotonergic neurons.^{48,49} Growing evidences also suggest that HDACi ameliorated deficits in synaptic plasticity, cognition, and stress-related behaviors in a wide range of neurologic and psychiatric disorders including AD, anxiety, and mood disorders.^{16,50,51} Furthermore, the serotonergic neurons in the raphe nucleus also innervate the medial prefrontal cortex (mPFC)⁵²; thus, it is reasonable to suggest that the loss of serotonergic neurons in the raphe nucleus can affect cognitive behavior. Evidence also suggests that anxiety traits exacerbate the cognitive impairments and hippocampal vulnerability in patients with AD.⁵³ Therefore, we suggest that the administration of MGCD0103 attenuated the anxiety and cognitive deficits induced by oligomeric A β_{25-35} via the raphe nucleus and limbic-related regions. The anxiolytic and attenuated cognitive deficit effects of MGCD0103 could provide an important benefit for both patients with AD and caregivers.

The systemic administration of MGCD0103 showed protective effects on the molecular alterations, including histone and nonhistone (α -tubulin) acetylation, A β deposition, tau phosphorylation, gliosis, and synapse-related protein changes, induced by oligomeric A β_{25-35} . Interestingly, we found that there was no significant difference in the acetylation of H3K9 and α -tubulin in the hippocampus of oligomeric A β_{25-35} - and saline-treated mice. However, chronic MGCD0103 treatment induced an increase in the acetylation of H3K9 and α -tubulin in the hippocampus of oligomeric A β_{25-35} -treated mice. These results are consistent with a previous study on APP/PS1 mice⁵⁴ and suggest that the memory deficits seen in acutely oligomeric A β_{25-35} -treated mice are not maintained by abnormalities in histone or nonhistone acetylation. However, the chronic administration of MGCD0103 caused elevations in histone and nonhistone acetylation in oligomeric A β_{25-35} -treated mice. Increased levels of H3K9 acetylation has also been observed in sodium butyrate-treated animals.⁵⁵ MGCD0103 also protected microtubule stability-related protein activity, including α -tubulin acetylation, S9GSK3 β phosphorylation, and tau protein phosphorylation at the T205 and S202 sites, against the effects of oligomeric A β_{25-35} treatment. Evidence

has shown that acetylated tubulin plays a critical role in microtubule stability at different ages or experimental conditions.⁵⁶ Previous studies also suggest that tau protein phosphorylation at both sites (S202 and T205) not only enhances polymerization but also increases filament formation sensitivity.⁵⁷ Therefore, treatment with MGCD0103 may protect the microtubule structure from the damage induced by oligomeric A β_{25-35} via increasing the levels of α -tubulin acetylation and pS9GSK3 β expression and decreasing the levels of phosphorylated tau at the T205 and S202 sites. Next, we further found that MGCD0103 treatment increased only the expression levels of synaptophysin and did not increase those of PSD95. These results are consistent with a previous study that assessed treatment with another HDACi, 4-phenylbutyrate.⁵⁴ In this study, oligomeric A β_{25-35} increased A β deposition and BACE1 expression and decreased IDE expression. MGCD0103 treatment increased only the levels of IDE, not NEP, under oligomeric A β_{25-35} conditions. Furthermore, evidence shows that the reduction in gliosis was not consistent in HDACi treatment.⁵⁸ However, treatment with MGCD0103 attenuated the gliosis induced by oligomeric A β_{25-35} .

Taken together, these results reveal MGCD0103 could be a potential therapeutic agent against AD.

ACKNOWLEDGMENTS

This work was partially supported by grants MOST 103-2325-B-003-003, MOST 104-2325-B-003-003, and MOST 105-2325-B-003-003 from the Ministry of Science and Technology (Taiwan). We thank the Molecular Imaging Core Facility of National Taiwan Normal University for the technical assistance under the auspices of the Ministry of Science and Technology.

CONFLICT OF INTEREST

The authors have no conflict of interests to declare.

ORCID

Hsiu Mei Hsieh-Li  <http://orcid.org/0000-0001-7435-0714>

REFERENCES

- Chen Z, Zhong C. Decoding Alzheimer's disease from perturbed cerebral glucose metabolism: implications for diagnostic and therapeutic strategies. *Prog Neurobiol*. 2013;108:21-43.
- Jeong S. Molecular and cellular basis of neurodegeneration in Alzheimer's disease. *Mol Cells*. 2017;40(9):613-620.
- Orgogozo JM, Gilman S, Dartigues JF, et al. Subacute meningoencephalitis in a subset of patients with AD after Abeta42 immunization. *Neurology*. 2003;61(1):46-54.
- Gravitz L. Drugs: a tangled web of targets. *Nature*. 2011;475(7355):S9-S11.
- Scharf S, Mander A, Ugoni A, Vajda F, Christophidis N. A double-blind, placebo-controlled trial of diclofenac/misoprostol in Alzheimer's disease. *Neurology*. 1999;53(1):197-201.

6. Zandi PP, Anthony JC, Khachaturian AS, et al. Reduced risk of Alzheimer disease in users of antioxidant vitamin supplements: the Cache County Study. *Arch Neurol*. 2004;61(1):82-88.
7. Huang HJ, Chen SL, Hsieh-Li HM. Administration of NaHS attenuates footshock-induced pathologies and emotional and cognitive dysfunction in triple transgenic Alzheimer's mice. *Front Behav Neurosci*. 2015;9:312.
8. Liu H, Le W. Epigenetic modifications of chronic hypoxia-mediated neurodegeneration in Alzheimer's disease. *Transl Neurodegener*. 2014;3(1):7.
9. Mah L, Binns MA, Steffens DC. Anxiety symptoms in amnesic mild cognitive impairment are associated with medial temporal atrophy and predict conversion to Alzheimer disease. *Am J Geriatr Psychiatry*. 2015;23(5):466-476.
10. Zawia NH, Lahiri DK, Cardozo-Pelaez F. Epigenetics, oxidative stress, and Alzheimer disease. *Free Radic Biol Med*. 2009;46(9):1241-1249.
11. de Ruijter AJ, van Gennip AH, Caron HN, Kemp S, van Kuilenburg AB. Histone deacetylases (HDACs): characterization of the classical HDAC family. *Biochem J*. 2003;370(Pt 3):737-749.
12. Cacabelos R, Torrellas C, Carrera I, et al. Novel therapeutic strategies for dementia. *CNS Neurol Disord Drug Targets*. 2016;15(2):141-241.
13. Gong HC, Wang YL, Wang HW. Epigenetic mechanisms of Alzheimer's disease and related drug research. *Yao Xue Xue Bao*. 2013;48(7):1005-1013.
14. Govindarajan N, Agis-Balboa RC, Walter J, Sananbenesi F, Fischer A. Sodium butyrate improves memory function in an Alzheimer's disease mouse model when administered at an advanced stage of disease progression. *J Alzheimers Dis*. 2011;26(1):187-197.
15. Sananbenesi F, Fischer A. The epigenetic bottleneck of neurodegenerative and psychiatric diseases. *Biol Chem*. 2009;390(11):1145-1153.
16. Abel T, Zukin RS. Epigenetic targets of HDAC inhibition in neurodegenerative and psychiatric disorders. *Curr Opin Pharmacol*. 2008;8(1):57-64.
17. Chuang DM, Leng Y, Marinova Z, Kim HJ, Chiu CT. Multiple roles of HDAC inhibition in neurodegenerative conditions. *Trends Neurosci*. 2009;32(11):591-601.
18. Blum KA, Advani A, Fernandez L, et al. Phase II study of the histone deacetylase inhibitor MGCD0103 in patients with previously treated chronic lymphocytic leukaemia. *Br J Haematol*. 2009;147(4):507-514.
19. Siu LL, Pili R, Duran I, et al. Phase I study of MGCD0103 given as a three-times-per-week oral dose in patients with advanced solid tumors. *J Clin Oncol*. 2008;26(12):1940-1947.
20. Fournel M, Bonfils C, Hou Y, et al. MGCD0103, a novel isotype-selective histone deacetylase inhibitor, has broad spectrum antitumor activity in vitro and in vivo. *Mol Cancer Ther*. 2008;7(4):759-768.
21. Klementiev B, Novikova T, Novitskaya V, et al. A neural cell adhesion molecule-derived peptide reduces neuropathological signs and cognitive impairment induced by Abeta25-35. *Neuroscience*. 2007;145(1):209-224.
22. Batlevi CL, Crump M, Andreadis C, et al. A phase 2 study of mocetinostat, a histone deacetylase inhibitor, in relapsed or refractory lymphoma. *Br J Haematol*. 2017;178(3):434-441.
23. Bumber Y, Younes A, Garcia-Manero G. Mocetinostat (MGCD0103): a review of an isotype-specific histone deacetylase inhibitor. *Expert Opin Investig Drugs*. 2011;20(6):823-829.
24. Pajouhesh H, Lenz GR. Medicinal chemical properties of successful central nervous system drugs. *NeuroRx*. 2005;2(4):541-553.
25. Denk F, Huang W, Sidders B, et al. HDAC inhibitors attenuate the development of hypersensitivity in models of neuropathic pain. *Pain*. 2013;154(9):1668-1679.
26. de Sousa LP, de Almeida RF, Ribeiro-Gomes FL, et al. Long-term effect of uncomplicated *Plasmodium berghei* ANKA malaria on memory and anxiety-like behaviour in C57BL/6 mice. *Parasit Vectors*. 2018;11(1):191.
27. Kobayashi S, Ishiguro K, Omori A, et al. A cdc2-related kinase PSSALRE/cdk5 is homologous with the 30 kDa subunit of tau protein kinase II, a proline-directed protein kinase associated with microtubule. *FEBS Lett*. 1993;335(2):171-175.
28. Flaherty DB, Soria JP, Tomasiewicz HG, Wood JG. Phosphorylation of human tau protein by microtubule-associated kinases: GSK3beta and cdk5 are key participants. *J Neurosci Res*. 2000;62(3):463-472.
29. Verkhatsky A, Sofroniew MV, Messing A, et al. Neurological diseases as primary gliopathies: a reassessment of neurocentrism. *ASN Neuro*. 2012;4(3):131-149.
30. Gomez-Isla T, Hollister R, West H, et al. Neuronal loss correlates with but exceeds neurofibrillary tangles in Alzheimer's disease. *Ann Neurol*. 1997;41(1):17-24.
31. Koffie RM, Meyer-Luehmann M, Hashimoto T, et al. Oligomeric amyloid beta associates with postsynaptic densities and correlates with excitatory synapse loss near senile plaques. *Proc Natl Acad Sci USA*. 2009;106(10):4012-4017.
32. Scheff SW, Price DA, Schmitt FA, Scheff MA, Mufson EJ. Synaptic loss in the inferior temporal gyrus in mild cognitive impairment and Alzheimer's disease. *J Alzheimers Dis*. 2011;24(3):547-557.
33. Haass C, Selkoe DJ. Soluble protein oligomers in neurodegeneration: lessons from the Alzheimer's amyloid beta-peptide. *Nat Rev Mol Cell Biol*. 2007;8(2):101-112.
34. Rowan MJ, Klyubin I, Wang Q, Hu NW, Anwyl R. Synaptic memory mechanisms: Alzheimer's disease amyloid beta-peptide-induced dysfunction. *Biochem Soc Trans*. 2007;35(Pt 5):1219-1223.
35. Klafki HW, Staufenbiel M, Kornhuber J, Wiltfang J. Therapeutic approaches to Alzheimer's disease. *Brain*. 2006;129(Pt 11):2840-2855.
36. Moon M, Choi JG, Nam DW, et al. Ghrelin ameliorates cognitive dysfunction and neurodegeneration in intrahippocampal amyloid-beta1-42 oligomer-injected mice. *J Alzheimers Dis*. 2011;23(1):147-159.
37. Wang X, Wang L, Xu Y, Yu Q, Li L, Guo Y. Intranasal administration of Exendin-4 antagonizes Abeta31-35-induced disruption of circadian rhythm and impairment of learning and memory. *Aging Clin Exp Res*. 2016;28(6):1259-1266.
38. Liu YM, Li ZY, Hu H, et al. Tenuifolin, a secondary saponin from hydrolysates of polygalasaponins, counteracts the neurotoxicity induced by Abeta25-35 peptides in vitro and in vivo. *Pharmacol Biochem Behav*. 2015;128:14-22.
39. Tang SS, Hong H, Chen L, et al. Involvement of cysteinyl leukotriene receptor 1 in Abeta1-42-induced neurotoxicity in vitro and in vivo. *Neurobiol Aging*. 2014;35(3):590-599.
40. Huang HJ, Liang KC, Chen CP, Chen CM, Hsieh-Li HM. Intrahippocampal administration of A beta(1-40) impairs spatial learning and memory in hyperglycemic mice. *Neurobiol Learn Mem*. 2007;87(4):483-494.
41. Kubo T, Nishimura S, Kumagai Y, Kaneko I. In vivo conversion of racemized beta-amyloid ([D-Ser 26]A beta 1-40) to truncated and toxic fragments ([D-Ser 26]A beta 25-35/40) and fragment presence in the brains of Alzheimer's patients. *J Neurosci Res*. 2002;70(3):474-483.
42. Reagan-Shaw S, Nihal M, Ahmad N. Dose translation from animal to human studies revisited. *FASEB J*. 2008;22(3):659-661.
43. Victoroff J, Lin FV, Coburn KL, Shilcutt SD, Voon V, Ducharme S. Noncognitive behavioral changes associated with Alzheimer's disease: Implications of neuroimaging findings. *J Neuropsychiatry Clin Neurosci*. 2017;30:14-21.
44. Zhao QF, Tan L, Wang HF, et al. The prevalence of neuropsychiatric symptoms in Alzheimer's disease: systematic review and meta-analysis. *J Affect Disord*. 2016;190:264-271.

45. Aletrino MA, Vogels OJ, Van Domburg PH, Ten Donkelaar HJ. Cell loss in the nucleus raphes dorsalis in Alzheimer's disease. *Neurobiol Aging*. 1992;13(4):461-468.
46. Weber T, Vogt MA, Gartside SE, et al. Adult AMPA GLUA1 receptor subunit loss in 5-HT neurons results in a specific anxiety-phenotype with evidence for dysregulation of 5-HT neuronal activity. *Neuropsychopharmacology*. 2015;40(6):1471-1484.
47. Linley SB, Olucha-Bordonau F, Vertes RP. Pattern of distribution of serotonergic fibers to the amygdala and extended amygdala in the rat. *J Comp Neurol*. 2017;525(1):116-139.
48. Balasubramanian D, Deng AX, Doudney K, Hampton MB, Kennedy MA. Valproic acid exposure leads to upregulation and increased promoter histone acetylation of sepiapterin reductase in a serotonergic cell line. *Neuropharmacology*. 2015;99:79-88.
49. Asaoka N, Nagayasu K, Nishitani N, et al. Inhibition of histone deacetylases enhances the function of serotonergic neurons in organotypic raphe slice cultures. *Neurosci Lett*. 2015;593:72-77.
50. Fischer A, Sananbenesi F, Wang X, Dobbin M, Tsai LH. Recovery of learning and memory is associated with chromatin remodelling. *Nature*. 2007;447(7141):178-182.
51. Weaver IC, Meaney MJ, Szyf M. Maternal care effects on the hippocampal transcriptome and anxiety-mediated behaviors in the offspring that are reversible in adulthood. *Proc Natl Acad Sci USA*. 2006;103(9):3480-3485.
52. Del Cid-Pellitero E, Garzon M. Medial prefrontal cortex receives input from dorsal raphe nucleus neurons targeted by hypocretin1/orexinA-containing axons. *Neuroscience*. 2011;172:30-43.
53. Zufferey V, Donati A, Popp J, et al. Neuroticism, depression, and anxiety traits exacerbate the state of cognitive impairment and hippocampal vulnerability to Alzheimer's disease. *Alzheimers Dement (Amst)*. 2017;7:107-114.
54. Cuadrado-Tejedor M, Ricobaraza AL, Torrijo R, Franco R, Garcia-Osta A. Phenylbutyrate is a multifaceted drug that exerts neuroprotective effects and reverses the Alzheimer's disease-like phenotype of a commonly used mouse model. *Curr Pharm Des*. 2013;19(28):5076-5084.
55. Silva PF, Garcia VA, Dornelles Ada S, et al. Memory impairment induced by brain iron overload is accompanied by reduced H3K9 acetylation and ameliorated by sodium butyrate. *Neuroscience*. 2012;200:42-49.
56. Baas PW, Rao AN, Matamoros AJ, Leo L. Stability properties of neuronal microtubules. *Cytoskeleton (Hoboken)*. 2016;73(9):442-460.
57. Rankin CA, Sun Q, Gamblin TC. Pseudo-phosphorylation of tau at Ser202 and Thr205 affects tau filament formation. *Brain Res Mol Brain Res*. 2005;138(1):84-93.
58. Lu WH, Wang CY, Chen PS, et al. Valproic acid attenuates microgliosis in injured spinal cord and purinergic P2X4 receptor expression in activated microglia. *J Neurosci Res*. 2013;91(5):694-705.

SUPPORTING INFORMATION

Additional supporting information may be found online in the Supporting Information section at the end of the article.

How to cite this article: Huang H-J, Huang H-Y, Hsieh-Li HM. MGCD0103, a selective histone deacetylase inhibitor, coameliorates oligomeric A β_{25-35} -induced anxiety and cognitive deficits in a mouse model. *CNS Neurosci Ther*. 2019;25:175-186. <https://doi.org/10.1111/cns.13029>